On the interplay between tungsten and tantalum atoms in Ni-based superalloys: An atom-probe tomographic and first-principles study

Yaron Amouyal,[1,a)] Zugang Mao,[1,b)] Christopher Booth-Morrison,[1,c)] and David N. Seidman[1,2,d)]
[1]*Department of Materials Science and Engineering, Northwestern University, 2220 Campus Drive, Evanston, Illinois 60208-3108, USA*
[2]*Northwestern University Center for Atom-Probe Tomography (NUCAPT), 2220 Campus Drive, Evanston, Illinois 60208-3108, USA*

(Received 12 December 2008; accepted 3 January 2009; published online 30 January 2009)

The partitioning behavior of W in a multicomponent Ni-based superalloy and in a ternary Ni–Al–W alloy is investigated using atom-probe tomography (APT) and first-principles calculations. APT observations indicate that whereas W partitions preferentially to the $\gamma'(L1_2)$-precipitates in the ternary alloy, its partitioning behavior is reversed in favor of the γ(fcc)-matrix in the multicomponent alloy. First-principles calculations of the substitutional formation energies of W and Ta predict that Ta has a larger driving force for partitioning to the γ' phase than W. This implies that Ta displaces W from the γ'-precipitates into the γ-matrix in multicomponent alloys. © *2009 American Institute of Physics*. [DOI: 10.1063/1.3073885]

High-temperature strength and creep resistance are the major prerequisites for materials for turbine blades of aerospace jet engines and land-based power generators. Ni-based superalloys are the ideal materials for these applications, owing to their unique two-phase, single-crystal microstructure, comprised of a high volume fraction of Ni_3Al-type $\gamma'(L1_2)$-precipitates that are dispersed in a γ(fcc)-matrix. Both phases contain refractory elements, which promote solid-solution strengthening of the γ-matrix (e.g., Mo, W, and Re) and the formation of γ'-precipitates (e.g., Ta).[1] The partitioning of elements to the γ- and γ'-phases in Ni-based superalloys determines the lattice parameter misfit at the coherent γ/γ' interface, which strongly correlates with the mechanical properties of the material at high temperatures.[2] The lattice parameter misfit is particularly sensitive to variations in the concentration of W on both sides of this heterophase interface due to its large atomic size.[1,3]

The partitioning behavior of W has been investigated in commercial multicomponent Ni-based superalloys using atom-probe tomography[4–8] (APT) and analytical electron microscopy.[9] These works indicate that W has a tendency to occupy the γ-matrix, yielding partitioning ratios ($K_i^{\gamma'/\gamma}$) slightly smaller than unity, where $K_i^{\gamma'/\gamma}$ is the ratio of the concentration of an element i in the γ'-precipitates to its concentration in the γ-matrix. To our knowledge, a value of $K_W^{\gamma'/\gamma}>1$ has not been reported for a multicomponent Ni-based superalloy. Studies of the partitioning behavior of W in model Ni-based alloys with less than four components by analytical transmission electron microscopy[3] and APT[10] have, however, reported $K_W^{\gamma'/\gamma}$ values ranging between 1.2 and 2.0. This difference between the $K_W^{\gamma'/\gamma}$ values measured for different Ni-alloys has not been explained on a scientific basis.

Herein, we present the results of APT analyses of the γ- and γ'-phases of both a ternary Ni–Al–W alloy and a multicomponent Ni-based superalloy to illustrate the reversal of the partitioning preference of W in multicomponent alloys. We hypothesize that the addition of Ta to Ni-superalloys is responsible for the reversal of the partitioning behavior of W. We prove this by employing first-principles calculations of the substitutional formation energy of W and Ta in the γ(fcc) and $\gamma'(L1_2)$ phases, in conjunction with APT studies.

A *multicomponent* Ni-14.6 Al-8.18 Cr-7.74 Co-1.95 Ta-0.95 Mo-2.31 W-1.47 Re-0.63 C-0.05 Hf (at. %) alloy and a *ternary* Ni-14 Al-3 W (at. %) alloy were directionally solidified employing the Bridgman technique to form ⟨100⟩-oriented single crystals.[11] APT microtip samples were prepared by electrochemical polishing.[12] Pulsed-laser APT was performed using local-electrode atom-probe (LEAP™) tomography,[13,14] at a specimen temperature of 40 ± 0.3 K, a 200 kHz pulse repetition rate, an energy of ~0.6 nJ pulse^{-1}, and a pressure $<5\times10^{-9}$ Pa. These experimental conditions were found to yield optimal compositional accuracy in a model Ni-based alloy.[15] Data analysis was performed using IVAS® (Imago Scientific Instruments), and compositional information was obtained with proximity histograms.[16]

Figure 1 displays typical three-dimensional (3D) APT reconstructions from both alloys, which contain the γ-and γ'-phases, separated by 8.2 at. % Cr and 12 at. % Al isoconcentration surfaces for the (a) multicomponent and (b) ternary alloys, respectively. For clarity, only the Ni, Al, and W distributions are displayed, showing the predominance of Ni (green) in the γ-phase and of Al (red) in the γ'-phase. Pronounced partitioning of W (represented as large spheres) to the γ'-phase in the ternary alloy is observed, with $K_W^{\gamma'/\gamma}=1.4\pm0.1$. Conversely, in the multicomponent alloy, W partitions to the γ-phase, resulting in $K_W^{\gamma'/\gamma}=0.92\pm0.06$. The calculated partitioning ratios are based on bulk analyses of $\sim10^5$ atoms in each of the γ-and γ'-phases. The other alloying additions to the multicomponent alloy (Cr, Co, Mo, Re, C, and Hf) exhibit pronounced partitioning to the γ-phase,

a)Electronic mail: y-amouyal@northwestern.edu.
b)Electronic mail: z-mao2@northwestern.edu.
c)Electronic mail: c-booth@northwestern.edu.
d)Author to whom correspondence should be addressed. Electronic mail: d-seidman@northwestern.edu. Tel.: +1-847-491-4391.

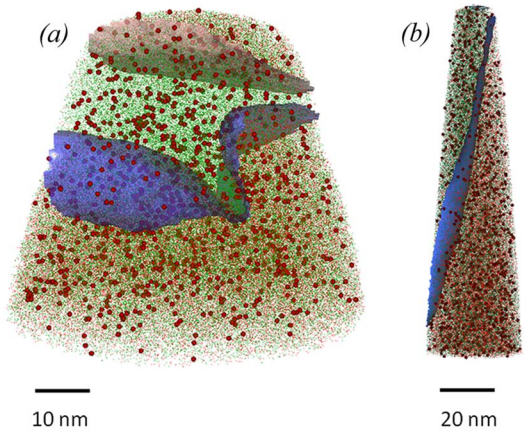

FIG. 1. (Color online) A 3D-APT reconstruction showing the γ(fcc)- and $\gamma'(L1_2)$-phases in the (a) multicomponent and (b) ternary alloys. The phases are separated by (a) 8.2 at. % Cr and (b) 12 at. % Al isoconcentration surfaces. Both reconstructions show 3% of the Ni (green), 8% of the Al (red), and 90% of the W (large red spheres) atoms detected for clarity.

except Ta, which is the *only* element that partitions strongly to the γ'-phase with $K_{Ta}^{\gamma'/\gamma}=18.4\pm0.4$. A very high value of $K_{Ta}^{\gamma'/\gamma}=10.25\pm0.07$ has also been observed in a model quaternary Ni-10.0 Al-8.5 Cr-2.0 Ta (at. %) alloy aged at 1073 K.[17,18]

What is the reason for the reversal of the partitioning behavior of W in multicomponent alloys? Since Ta is the only element that partitions preferentially to the γ'-precipitates, and given that both W and Ta occupy the same Al substitutional sublattice sites in the $\gamma'(L1_2)$-phase,[4,17,19] we can reasonably assume that Ta is responsible for this effect, by displacing W from the Al-sublattice of the γ'-precipitates into the γ-matrix. To illustrate this effect, the W and Ta compositional profiles across the γ/γ' interfaces of the ternary and multicomponent alloys, determined by 3D-APT, are shown in Fig. 2. The concentration of W on the γ'-precipitate side of the interface in the Ni–Al–W alloy (empty circles) is considerably larger

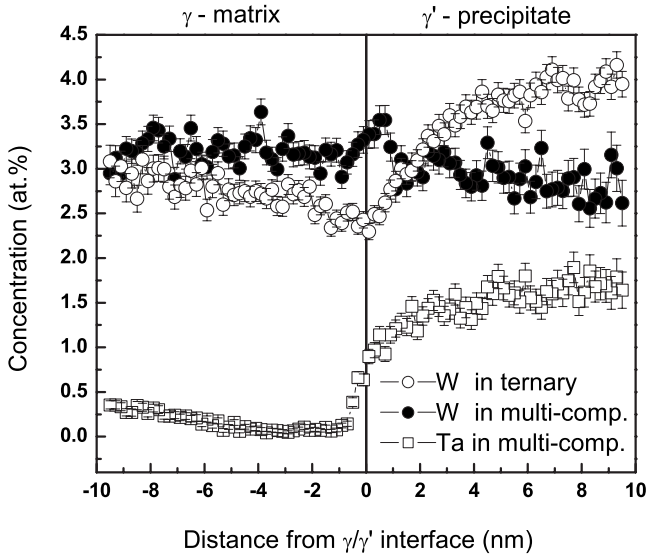

FIG. 2. The experimental APT concentration profiles of W across the γ/γ' interfaces of the ternary Ni–Al–W alloy (empty circles) and the multicomponent alloy (full circles). For comparison, the Ta concentration profile in the multicomponent alloy is plotted as empty squares. All profiles are plotted with respect to the isoconcentration surfaces shown in Fig. 1.

than on the γ-side. In the multicomponent alloy, however, this trend is reversed (full circles). The strong partitioning of Ta to the γ'-phase in the multicomponent alloy (empty squares) suggests that Ta has a stronger affinity for the Al-sublattice sites of the γ'-precipitates than W does, leading to the displacement of W to the γ'-matrix.

To test this hypothesis quantitatively, we performed first-principles calculations of the substitutional formation energy of W and Ta in the γ(Ni, fcc) phase as well as at the Ni-and Al-sublattice sites of the $\gamma'(Ni_3Al, L1_2)$ phase at 0 K. The first-principles calculations were performed using the plane wave pseudopotential total energy method with the general gradient approximation, as implemented in the Vienna *ab initio* simulation package (VASP).[20–22] The lattice parameter of the relaxed Ni_3Al structure was calculated to be 0.3566 nm, in agreement with the experimental room temperature value of 0.3570 nm.[1] A model W- and Ta- microalloyed Ni–Al system was built to simulate the experimental conditions. Three supercells were simulated. Each was divided by one of the {100}, {110}, and {111} heterophase interfaces, and the two-halves of the supercells were occupied by the γ-Ni and γ'-Ni_3Al phases, respectively. Projector augmented-wave pseudopotentials[23] were employed with an energy cutoff of 300 eV for plane waves in optimized $8\times8\times1$ Monkhorst–Pack k-point grids. The ground-state atomic geometries of the structures were obtained by minimizing the total energy using Hellman–Feynman forces with a cutoff value of 5 meV nm^{-1}. The total energies of the relaxed structures were converged with respect to an energy cutoff of 0.02 meV $atom^{-1}$. The substitutional formation energies of W and Ta were calculated when W or Ta was placed at different sites close to each of the three simulated interfaces. The construction of these interfaces and the locations of these sites are described elsewhere.[19] The calculations are described by the relationships:

$$E_{M\rightarrow \mathrm{Ni\ or\ Al}}=[(E^{\mathrm{tot}}_{M\ in\ \gamma'}+n_{\mathrm{Ni\ or\ Al}}\mu_{\mathrm{Ni\ or\ Al}})-(E^{\mathrm{tot}}+n_M\mu_M)]/n_M \quad (1)$$

for the γ'-precipitate, and

$$E_{M\rightarrow \mathrm{Ni}}=[(E^{\mathrm{tot}}_{M\ in\ \gamma}+n_{\mathrm{Ni}}\mu_{\mathrm{Ni}})-(E^{\mathrm{tot}}+n_M\mu_M)]/n_M \quad (2)$$

for the γ-matrix. In this notation, M represents the substitutional atom W or Ta, and n_i is the number of i atoms. E^{tot} is the total energy of the supercell, including the interface, prior to substitution. $E^{\mathrm{tot}}_{M\ in\ \gamma'}$ and $E^{\mathrm{tot}}_{M\ in\ \gamma}$ are the total energies of the M-microalloyed supercell calculated for substitution in the γ' or γ, respectively. γ denotes a fcc-based substitutional solid solution of Ni; γ' has several alternative structural forms: $(Ni_xM_{1-x})_3Al$ for substitution on the Ni-sublattice and $Ni_3(Al_yM_{1-y})$ for substitution on the Al-sublattice. μ_i represents the chemical potential of the bulk pure element i, and is calculated assuming same cell symmetry. The values of μ_i are −5.432, −3.697, −12.644, and −11.478 eV $atom^{-1}$ for Ni, Al, W, and Ta, respectively. Additionally, the average atomic forces and displacements due to substitution at the first nearest-neighbor sites were calculated. No atomic force was measured for relaxed bulk, either $\gamma'(Ni_3Al)$ or γ(Ni), prior to site substitution. While the substitutional formation energy, $E_{M\rightarrow \mathrm{Ni\ or\ Al}}$, indicates the preference of M at specific sublattice sites originating from interatomic electronic interactions, the force and displacement terms yield the elastic energy due

TABLE I. The substitutional formation energies of W and Ta in the γ(fcc)-matrix, and at both the Ni- and Al-sublattice sites of the $\gamma'(L1_2)$-precipitates. The average atomic displacements and forces caused by these substitutions are also listed.

Phase	Substitutional site	$E_{M\rightarrow \text{Ni or Al}}$ (eV atom^{-1})	Average atomic force (meV Å^{-1})	Average atomic displacement (Å)
γ(fcc)	Ni_xW_{1-x}	−0.325	25.67	0.0528
	Ni_yTa_{1-y}	−0.248	13.65	0.0315
$\gamma'(L1_2)$	$(Ni_xW_{1-x})_3Al$	0.133	27.64	0.0668
	$Ni_3(Al_yW_{1-y})$	−0.426	16.92	0.0455
	$(Ni_xTa_{1-x})_3Al$	0.033	15.77	0.0463
	$Ni_3(Al_yTa_{1-y})$	−0.473	9.98	0.0222

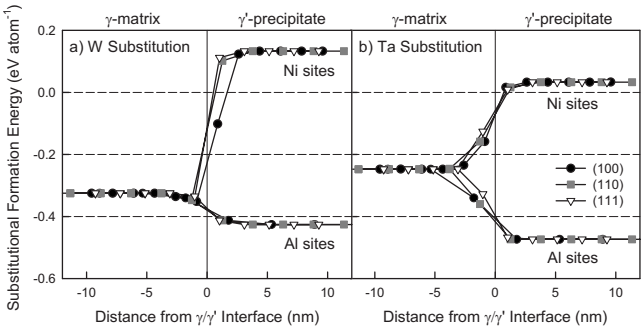

FIG. 3. The substitutional formation energies of (a) W and (b) Ta atoms as a function of the distance from the {100}, {110}, and {111} γ/γ' interfaces, obtained using first-principles calculations performed in a model $Ni(\gamma)/Ni_3Al(\gamma')$ system.

to site substitution. The latter have a second-order effect when compared to the electronic interactions, signifying the likelihood of substitution in both phases. The bulk values resulting from these first-principles calculations appear in Table I.

The values of the substitutional formation energies shown in Table I clearly indicate that W and Ta atoms prefer to occupy the Al-sublattice sites of the γ'-precipitates. This result is in agreement with previous experimental data.[4,17,19] The substitutional formation energies of both W and Ta in the γ-matrix are greater than in the γ'-precipitates, indicating a clear preference of both elements for the γ'-precipitates, resulting in $K_i^{\gamma'/\gamma}$ values greater than unity. Moreover, the substitution of Ta at Al sites in the γ'-precipitates is more energetically favorable than that of W. The opposite trend, however, is observed in the γ-matrix. Furthermore, the substitution of W and Ta at the Al-sublattice sites results in smaller values of the atomic forces and displacements than substitution of W and Ta at the Ni-sublattice sites. The atomic forces and displacements associated with substitution in the γ-matrix have intermediate values. All the results of the calculations support firmly the hypothesis that the addition of Ta to multicomponent alloys leads to the displacement of W from the Al-sublattice sites of the γ'-precipitates, and into the γ-matrix. This displacement effect results in an inversion of the partitioning ratio of W from $K_W^{\gamma'/\gamma}>1$ to $K_W^{\gamma'/\gamma}<1$, as demonstrated by the results presented in Fig. 2. Figure 3 is a graphic representation of the substitutional formation energies of (a) W and (b) Ta as a function of their distance from the {100}, {110}, or {111} interface.

The results clearly indicate the existence of an energetic driving force for the partitioning of both elements to the γ'-precipitates. The driving force for the partitioning of Ta to the γ'-precipitates of 0.225 eV atom^{-1} is about twice as large as the value of W of 0.101 eV atom^{-1}. The difference in the driving force for partitioning is responsible for the reversal of the partitioning ratio of W in alloys that also contain Ta. We note that the partitioning behavior is the same for all crystallographic planes separating the γ'- and γ-phases, keeping in mind that the set of {100}, {110}, and {111} planes is representative of the space of crystallographic orientations.

In summary, we find that W prefers to partition strongly to the γ' -phase in a model ternary Ni–Al–W alloy, while this behavior is reversed in multicomponent Ni-based alloys. This effect is explained by first-principles calculations of the substitutional formation energies of W and Ta in both phases, which reveal that the driving force for the partitioning of Ta to the γ' -phase is nearly twice as large as the value calculated for W. These findings imply that Ta atoms replace W atoms in the γ'-precipitates, leading to a reversal of the partitioning behavior of W between the two phases.

This research was implemented in support of MEANS II AFOSR Grant No.FA9550-05-1-0089 and of the National Science Foundation (NSF) under Grant No. DMR-0804610 for Z.M. and C.B.-M. Y.A. wishes to acknowledge the Marie Curie IOF (CEC FP7). Dr. L. Graham and Prof. T. Pollock are kindly thanked for supplying alloys. The LEAP tomograph was purchased with funding from the NSF-MRI and ONR-DURIP programs. The authors thank Dr. D. Isheim for managing NUCAPT and for helpful discussions.

[1] R. C. Reed, *The Superalloys: Fundamentals and Applications* (Cambridge University Press, New York, 2006), p. 372.
[2] R. D. Rawlings and A. E. Staton-Bevan, J. Mater. Sci. **10**, 505 (1975).
[3] A. Volek, F. Pyczak, R. F. Singer, and H. Mughrabi, Scr. Mater. **52**, 141 (2005).
[4] D. Blavette, E. Cadel, C. Pareige, B. Deconihout, and P. Caron, Microsc. Microanal. **13**, 464 (2007).
[5] R. C. Reed, A. C. Yeh, S. Tin, S. S. Babu, and M. K. Miller, Scr. Mater. **51**, 327 (2004).
[6] T. Yokokawa, M. Osawa, K. Nishida, T. Kobayashi, Y. Koizumi, and H. Harada, Scr. Mater. **49**, 1041 (2003).
[7] K. E. Yoon, D. Isheim, R. D. Noebe, and D. N. Seidman, Interface Sci. **9**, 249 (2001).
[8] R. Balamuralikrishnan, R. Sankarasubramanian, M. P. Pathak, K. Muraleedharan, and N. Das, *Superalloys 2008* (The Minerals, Metals, and Materials Society, Seven Springs, PA, 2008), p. 993.
[9] T. M. Pollock and S. Tin, J. Propul. Power **22**, 361 (2006).
[10] C. K. Sudbrack, D. Isheim, R. D. Noebe, N. S. Jacobson, and D. N. Seidman, Microsc. Microanal. **10**, 355 (2004).
[11] S. Tin and T. M. Pollock, Metall. Mater. Trans. A **34A**, 1953 (2003).
[12] B. W. Krakauer and D. N. Seidman, Rev. Sci. Instrum. **63**, 4071 (1992).
[13] D. N. Seidman, Annu. Rev. Mater. Sci. **37**, 127 (2007).
[14] T. F. Kelly and M. K. Miller, Rev. Sci. Instrum. **78**, 031101 (2007).
[15] Y. Zhou, C. Booth-Morrison, and D. N. Seidman, Microsc. Microanal. **14**, 571 (2008).
[16] O. C. Hellman and D. N. Seidman, Mater. Sci. Eng., A **327**, 24 (2002).
[17] C. Booth-Morrison, Z. Mao, R. D. Noebe, and D. N. Seidman, Appl. Phys. Lett. **93**, 033103 (2008).
[18] C. Booth-Morrison, R. D. Noebe, and D. N. Seidman, Acta Mater. **57**, 909 (2009).
[19] Y. Amouyal, Z. Mao, and D. N. Seidman, Appl. Phys. Lett. **93**, 201905 (2008).
[20] G. Kresse and J. Furthmuller, Comput. Mater. Sci. **6**, 15 (1996).
[21] G. Kresse and J. Furthmueller, Phys. Rev. B **54**, 11169 (1996).
[22] G. Kresse and J. Hafner, Phys. Rev. B **49**, 14251 (1994).
[23] G. Kresse and D. Joubert, Phys. Rev. B **59**, 1758 (1999).